Optical observations of gamma-ray bursts

J. Hjorth[a], E. Pian[bc] and J. P. U. Fynbo[d]

[a]Niels Bohr Institute, Astronomical Observatory, University of Copenhagen, Juliane Maries Vej 30, DK–2100 Copenhagen Ø, Denmark

[b]INAF, Astronomical Observatory of Trieste, Via G.B. Tiepolo 11, I–341 31 Trieste, Italy

[c]CNR-IASF, Via. P. Gobetti 101, I–40129 Bologna, Italy

[d]Institute of Physics and Astronomy, University of Aarhus, DK–8000 Århus C, Denmark

We briefly review the status and recent progress in the field of optical observations of gamma-ray burst afterglows. We will focus on the fundamental observational evidence for the relationship between gamma-ray bursts and the final evolutionary phases of massive stars. In particular, we will address (i) gamma-ray burst host galaxies, (ii) optically dark gamma-ray burst afterglows, (iii) the gamma-ray burst–supernova connection, and (iv) the relation between X-ray flashes, gamma-ray bursts, and supernovae.

1. INTRODUCTION

The detection and monitoring of gamma-ray burst (GRB) afterglows at many wavelengths has boosted our knowledge of these high energy sources, so that the last seven years since first afterglow detection have witnessed an incomparably larger progress in the understanding of GRB physics than afforded by gamma-ray observations of the prompt events only [1]. The basic ingredient of this success has been the determination of the GRB distance scale, made possible by redshift measurements through accurate afterglow spectroscopy and deep optical and infrared imaging and spectroscopy of host galaxies. The cosmological distance scale of GRBs has thus been firmly established[1]. As is well known, BeppoSAX played a crucial role in this scientific revolution, with the discovery of the first X-ray afterglow [2] and resulting accurate localization of GRBs up to the end of the mission.

The redshift distribution for 35 GRBs (as of December 2003) is shown in Fig. 1. The mean and median redshifts are 1.1 and 1.4 respectively. At such redshifts, GRBs have energy outputs of the order of $\sim 10^{52}$–10^{53} erg, assuming the radiation is emitted isotropically (Fig. 1). These energies are reminiscent of those emitted by supernovae (SNe), although at least one order of magnitude larger. This has reinforced the hypothesis that GRBs are originated in powerful SN explosions. Specifically, very massive stars should end their lives via core collapse by leaving behind a 2–3 $M_\odot$ black hole [4]. Part of the envelope promptly forms an accretion disk which feeds a (probably two-sided) jet. The rotational energy extracted from the black hole is carried along the jet as a relativistic outflow which produces the GRB via internal hydrodynamical shocks and the multiwavelength afterglow via interaction of the decelerating blast wave with the circumstellar medium (external shock, [5]).

An important consequence of this scenario is that GRBs are expected to trace massive star formation, so that their distribution as a function of redshift should be correlated with the history of star formation in the Universe.

Observations of GRB afterglows and their host galaxies from radio to X-ray frequencies have provided various independent suggestions that GRBs

[1]We refer here to long GRBs, i.e., those with duration larger than $\sim$2 seconds, as opposed to sub-second GRBs, which represent $\sim$30% of the GRB population and have no detected counterparts at energies lower than the gamma-rays [3].

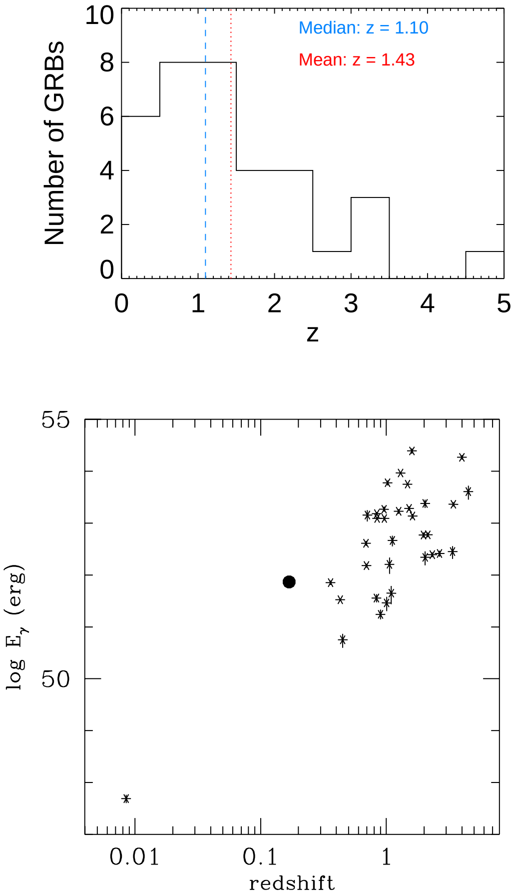

Figure 1. *Top:* The distribution of GRB redshifts. The median and mean redshifts are 1.1 and 1.4. For more recent bursts (2002–2003) the median and mean redshifts are 1.5. *Bottom:* Isotropic gamma-ray output of GRBs vs. redshift. The filled circle represents GRB 030329 (see Sect. 3).

indeed tend to explode in sites where active star formation is taking place. Many of these are related to the properties of the GRB host galaxies (see Sect. 2). Another clue comes from the detection of metal lines in the X-ray afterglows, both in emission and absorption [6–12]. These are interpreted as signatures of a medium enriched by explosive nucleosynthesis, such as occurring in supernova events. Moreover, for GRB 021004, optical spectroscopy of the afterglow revealed absorption lines with multiple velocity components, indicating the presence of shells around a massive progenitor star [13,14]. However, the strongest indication that GRBs are related to a massive star population comes from the direct connection between some GRBs and SN features (Sect. 3). Finally, in Sect. 4 we discuss the possible connection between SNe and X-ray Flashes, a new class of objects discovered by BeppoSAX [15].

2. GRB HOST GALAXIES

In almost all cases when the position of an afterglow has been determined to arcsecond precision (through imaging in the optical, radio, or X-rays with the Chandra or XMM-Newton satellites) a galaxy has been detected at angular distance not exceeding a few arcseconds from the afterglow. This is usually identified with the GRB host galaxy, and generally spectroscopy of both afterglow and galaxy confirm the association. Accurate astrometry of the point-like afterglow source indicates that the projected distance of the GRB from the center of its host is on average a fraction of an arcsecond, but almost never consistent with zero [16,17]. This excludes that GRBs are caused by nuclear events, and points to their association with the peripheral regions of the host stellar disks, where most of the star formation takes place.

The morphologies of GRB host galaxies are often irregular or disky, typical of late-type galaxies, where most of the star formation is occurring. In some cases they are found to belong to small groups or even weakly interacting systems, an environmental characteristic thought to also favour or trigger star formation [18–22].

GRB host galaxies are generally underluminous and have blue colors [23,24], indicative of ongoing intense star formation. For those having extensive broad-band optical and near-infrared photometry, the modeling of the spectral energy distribution is well accounted for by starburst template spectra [25–27]. In many cases there are strong emission lines considered to be star formation indicators ([O II], [O III], Lymanα, Balmer and Paschen series, [Ne III]) [27–31]. In particular, the [O II] line equivalent widths measured for GRB hosts are among the largest in an unbiased sample such as the Hubble Deep Field [32]. The star formation rates derived from the spectral continua of host galaxies or from the emission line strengths range between 0.1 to 10 $M_\odot$/yr, remarkable for small and underluminous galaxies, although not exceptionally high. The specific star formation rates are, however, very high compared to starburst galaxies in the Hubble Deep Fields (Fig. 2). Moreover, these are likely to represent underestimates of the true values, due to intrinsic extinction affecting the continuum and line fluxes, emitted at UV restframe wavelengths. The star formation rate estimates based on radio and millimeter observations can exceed those derived in the optical by as much as a factor 100 [34–36], although it is not clear why sub-millimeter host galaxies such as those of GRB 000210 and GRB 000418 appear to be typical faint blue galaxies with a young, unextincted stellar population [25,26].

That significant intrinsic obscuration must occasionally be present is indicated by the afterglow optical and soft X-ray spectra, often affected by small additional extinction on top of the Galactic one. This however may be local to the GRB. In fact, a gas- and dust-rich close environment could cause many GRB counterparts to be unobservable at optical frequencies. Whether the optical "darkness" of this fraction of afterglows is due to a higher density of the circumburst medium with respect to optically bright counterparts is not clear. The difference may in fact also arise from the geometry of the source itself: a more collimated jet may have sufficient power to efficiently destroy the surrounding dust and carve a path for optical light to reach the observer, while less collimated, and thus less powerful, jets would leave the dust grains unaltered, and optical light would be absorbed [37]. In conclusion, although the role played by dust in "dark" GRBs (see Fig. 3 for a classification of BeppoSAX GRBs) is still unclear, there is little doubt about its presence, which again points to a star forming environment.

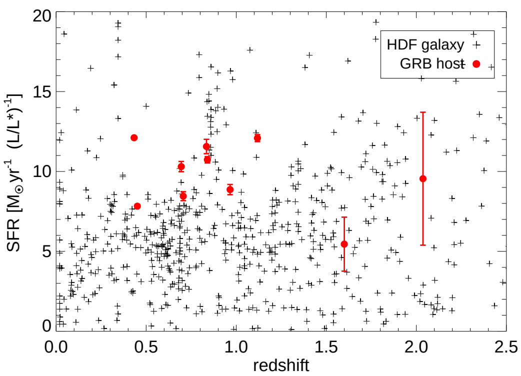

Figure 2. Specific UV star-formation rates (star-formation rates normalized to the total luminosity) for a complete sample of GRB host galaxies with $R < 25.3$. These are compared to specific star-formation rates for starburst galaxies in the Hubble Deep Fields. GRB host galaxies have on average larger specific star-formation rates (from [33]).

3. THE GRB–SN CONNECTION

While the hypothesis that GRBs originate in SN explosions dates from the time of GRB discovery [39], only in the last five years could this scenario be confirmed observationally, at least for some GRBs. The detection of a peculiar Type Ic SN, SN 1998bw, in the error box of GRB 980425 has been regarded as a strong indication of causality between the two events [40–43]. However, due to the remarkably short distance to the SN ($z = 0.0085$) as compared to that of the majority of GRBs with measured redshift (Fig. 1), and to the lack of a "classical" multiwavelength afterglow, the association between GRB 980425 and

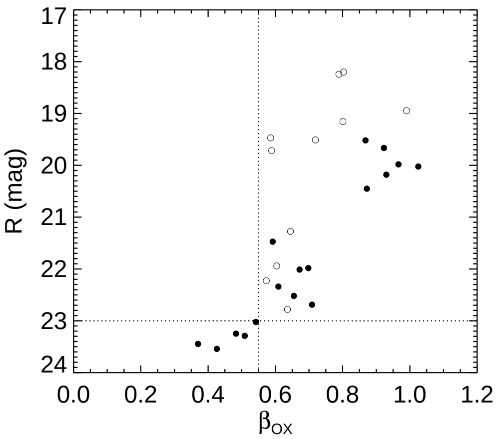

Figure 3. BeppoSAX GRBs from [38]. Filled circles are GRBs with no detected afterglow, open circles are GRBs with a detected optical afterglow. The R-band magnitude and the optical-to-X-ray spectral index, β_{OX}, has been computed at 11 hours after the GRB. Dark GRBs are those that are both dim (faint in R, e.g., $R > 23$ @ 11 hours) and optically subluminous (e.g., a spectral index smaller than expected for a fireball model with $\nu < \nu_c$ and $p < 2.2$, i.e., $\beta_{\mathrm{OX}} < 0.55$).

SN 1998bw has been controversial. A number of GRB optical/NIR counterparts clearly exhibited re-brightenings in their light curves, which have been attributed to the contribution of an underlying SN [44–59]. However, detailed spectroscopy during the re-brightening was only rarely feasible owing to the faintness of the fluxes and/or the contamination from the host galaxy, and when accomplished the presence of a SN could not be confirmed.

A bright optical afterglow was identified for the GRB of 29 March 2003 [60–62]. Its redshift ($z = 0.1685$) was very low with respect to the average of other GRBs (Fig. 1), but higher than GRB 980425. This "intermediate" redshift, but truly cosmological, GRB ought to be the Rosetta stone of long GRBs progenitors, since if a SN was present it would show up prominently, due to its relative proximity. Spectroscopic campaigns started shortly after GRB detection, and SN absorption features superposed on the power-law afterglow spectrum were revealed within one week. These signatures became increasingly evident with time as the non-thermal component decayed, and were strikingly reminiscent of those exhibited by SN 1998bw (Fig. 4). The presence of a Type Ic SN (SN 2003dh) was first announced by Stanek et al. [63]. Spectroscopy with the ESO Very Large Telescope (VLT) at epochs ranging from 4 days to 1 month after the GRB allowed Hjorth et al. [30] to follow the spectral evolution of the SN, to reconstruct the SN 2003dh light curve through subtraction of the non-thermal afterglow component from the observed fluxes, and to map the temporal evolution of the photospheric velocity. This is $\sim 0.1c$ at about 1 week after the GRB, similar to the values reached in SN 1998bw, and is indicative of extreme kinematic conditions (Fig. 5).

To reproduce these conditions, the models imply very high explosion energies, of the order of $\sim 10^{52}$ erg (in spherical symmetry), which is more than an order of magnitude larger than the kinetic energy of normal SNe [64–66]. Also, for both SN 1998bw and SN 2003dh, modelling of the light curve yielded the result that the mass of radioactive ^{56}Ni synthesised – which is necessary to produce the luminosity of the SNe – was much

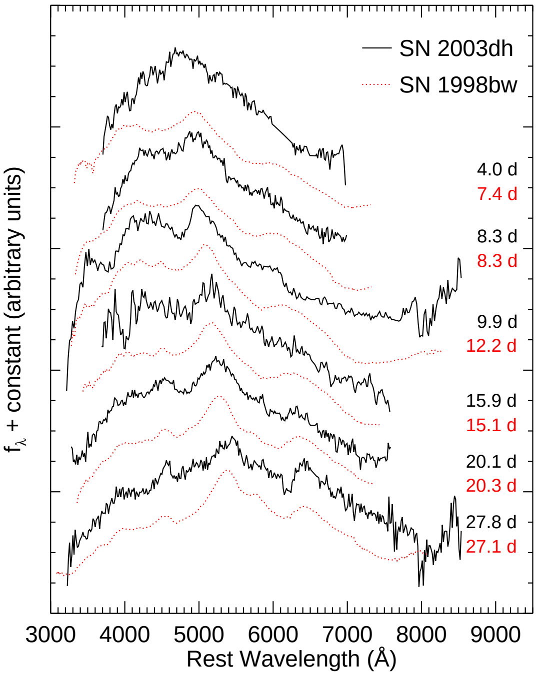

Figure 4. Comparison of the spectral evolution of SN 2003dh and SN 1998bw. Solid curves indicate spectra of SN 2003dh obtained through subtraction of the afterglow and host galaxy spectrum from the observed VLT spectra. Dotted curves indicate spectra of SN 1998bw taken at similar epochs (from [30]).

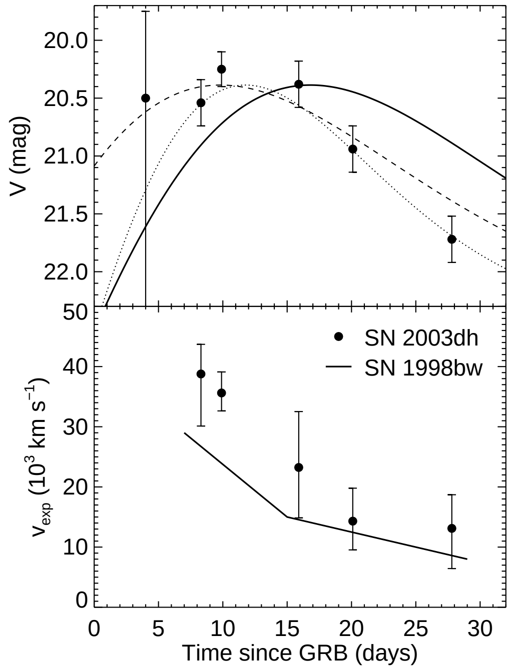

Figure 5. *Top:* V-band light curve of SN 2003dh at restframe since GRB 030329 (filled circles). The solid line represents the brightness of SN 1998bw as it would have appeared in the V band at $z = 0.168$ as a function of time (restframe) since GRB 980425. Dashed line: as for the solid line but shifted 7 days earlier. Such an evolution may be expected if the SN exploded 7 days before the GRB. For SN 2003dh, however, this is inconsistent with its spectral evolution. Dotted line: as for solid line, but evolution speeded up by multiplying time by 0.7 (i.e., the velocity ratio of SN 2003dh to SN 1998bw). A faster rise and decay may be expected in asymmetric models in which an oblate SN is seen pole-on. A 0.2 mag extinction is assumed for SN 1998bw and none for SN 2003dh. *Bottom:* Si II λ6355 expansion velocities as a function of time (restframe) of SN 2003dh (filled circles) and SN 1998bw (solid line) (from [30]).

larger than in normal core-collapse SNe (0.5 and 0.35 $M_\odot$, respectively, vs. 0.1 $M_\odot$). In these powerful SNe, also dubbed “hypernovae” [67,64], the kinetic energy may be overestimated if the explosions were asymmetric and we observed the SNe near the direction of highest energy output, as is possible since we observed the GRBs.

Other SNe Ic which exhibited broad lines typical of hypernovae have been studied [68–70]. Although these SNe apparently were not associated with a GRB, this could be due to an unfavourable orientation and/or a less energetic explosion. All of these objects have in common a higher-than-normal kinetic energy and a large progenitor mass ($> 20 M_\odot$), suggesting that these events may be related to the formation of a black hole.

This is in line with the theory for the birth of GRBs, which favours Type Ib/c SNe as GRB progenitors [4,71]. SNe Ib/c have smaller envelopes than SNe II, making it easier for relativistic jets to break out. Jets may originate in the collapse of a neutron star to a black hole, which points to massive progenitors.

4. X-RAY FLASHES

Heise et al. [15] first described a new class of events detected by WFC, but not the GRBM, on BeppoSAX. Such X-ray flashes (XRFs) may (or may not) have a similar origin as GRBs.

The two first XRFs precisely localized by BeppoSAX were XRF 011030 and XRF 020427. For these, X-ray afterglows were detected and localized to arcsec precision by Chandra X-ray Observatory. HST observations has revealed candidate blue $R \sim 25$ host galaxies for both of these XRFs, typical of GRB host galaxies. The galaxies are not at very high redshift (see [72]). The first XRF with a candidate optical afterglow was the HETE-2 XRF 020903. A bright galaxy with complex morphology coincident with the optical/radio transient was found at $z = 0.25$ [73].

The best studied XRF to date is the HETE-2 X-Ray Flash of July 23, 2003 [74]. The R-band lightcurve from a few hours to about 70 days after the explosion is shown in Fig. 6. The decay curve is consistent with being very flat during the first 24 hr after the burst, perhaps indicating an off-axis GRB [75]. Around 1 day after the burst the decay slope steepens to about -2 and it remains so for the following 4–5 days. Around a week after the burst the decay curve starts to deviate from the fast decay and it then quickly rises to a secondary maximum, peaking at around 16 days, followed by a new steep decay. The bump emission with an extrapolation of the afterglow lightcurve subtracted is shown in the middle panel of Fig. 6.

Spectroscopic observations indicate an upper limit to the redshift of about $z = 2.3$ from the lack of Lyα absorption. Multicolor imaging was secured on four epochs. Initially, the afterglow spectral energy distribution is well described by a $\beta \approx -1$ power-law over the full range from the U-band to the K-band (right panel of Fig. 6). During the bump phase the spectral energy distribution starts to deviate strongly from a power-law shape due to a strong decrease in the flux in the bluest bands.

In a sense the situation for XRF 030723 is opposite to that of GRB 030329. For GRB 030329 the lightcurve did not show a strong bump apparently due to a late break in the afterglow lightcurve that by coincidence balanced out the extra emission from the SN. On the other hand the spectroscopic evidence was unambiguous. For XRF 030723 the photometry shows the most significant late time bump ever detected in an afterglow lightcurve at the time expected for an underlying supernova, but the spectroscopic evidence is more unclear. Nevertheless, it is clear that a SN 1998bw lightcurve is inconsistent with the data at any redshift. So far the best match found is for a SN similar to the type Ic SN 1994I, which had a very early peak time and a rather narrow peak in its lightcurve, at a redshift around $z \approx 0.6$ (Fig. 6, middle panel). Interestingly, a SN similar to SN 1994I has also been proposed to be associated with GRB 021211 [55].

5. OUTLOOK

The study of GRB multiwavelength afterglows and host galaxies has offered an unprecedented insight into GRB phenomenology, demographics and progenitor population. The exploratory work accomplished by satellites and by ground-

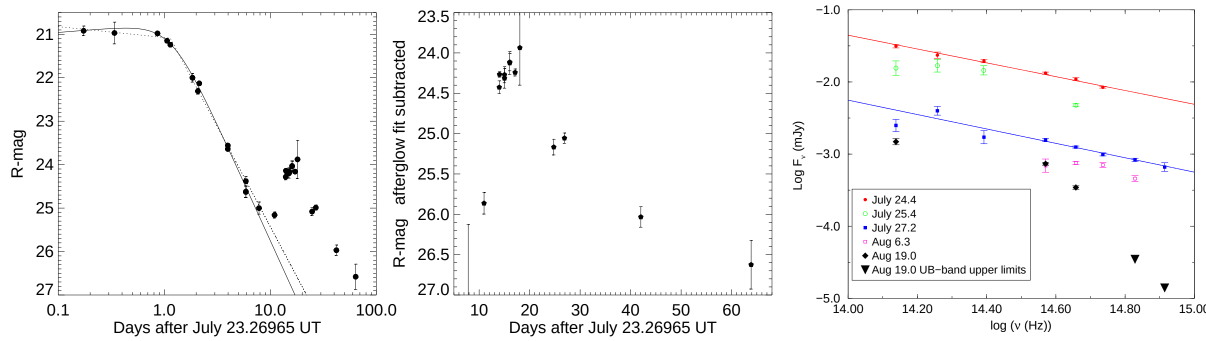

Figure 6. Lightcurve and spectral energy distribution of the optical afterglow of XRF 030723. *Left:* R-band lightcurve. *Middle:* Bump lightcurve after subtraction of the power-law afterglow decay. *Right:* evolution of the spectral energy distribution showing a marked attenuation of the blue part of the spectrum after the peak of the lightcurve bump (from [74]).

based optical and radio telescopes will soon be followed by a more systematic approach by dedicated spacecrafts and instruments.

The Swift probe, to be launched in mid 2004, will increase the rate of prompt and accurate GRB localizations by nearly an order of magnitude with respect to present, and will bring GRB science into the domain of statistics. Moreover, it will open the very early afterglow epochs (minutes to hours after GRB explosion) to our view and investigation. In this sense, robotic telescopes, reacting promptly and efficiently to Swift alerts, will play a crucial role in detecting the initial optical and NIR flashes accompanying GRBs. These are expected, at least in a large fraction of cases, to be extremely bright [76] and to represent excellent probes of the circumstellar as well as of the intervening medium, to test progenitor physics and cosmology, respectively.

To perform these tests, one will need accurate and good resolution spectroscopy from UV to NIR wavelengths executed in a timely fashion. These can be done with an instrument similar to the Echellette Spectrograph and Imager mounted on the Keck telescope, with possibly farther extension into the NIR range. Such a spectrograph ("X-shooter") is being planned for the second generation of VLT instruments. Its main goals in the GRB field will be 1) routinely measure GRB redshifts from spectroscopy of their afterglows, to increase the number of known distances and build a GRB luminosity function; 2) monitor time-dependent variations of the equivalent widths of weak absorption lines in afterglows, to test the progenitor models and GRB formation sites; 3) implement a spectroscopic survey of GRB host galaxies by which we will measure redshifts, emission line intensities and broad band energy distributions, and thus catalog their distances and properties.

These new tools will allow us to tackle the many still unsolved problems of GRB physics more effectively than possible before and with a high expectation of exciting progress.

6. ACKNOWLEDGEMENTS

We thank Lise Christensen and Páll Jakobsson for permission to reproduce Figures 1 and 2 prior to publication. Part of the work presented in this article is the result of an observing program implemented at ESO telescopes by the GRACE consortium, which is here acknowledged for years of fruitful collaboration.

REFERENCES

1. J. Fishman and C. Meegan, ARA&A, 33, 415 (1995).

2. E. Costa et al., Nature, 387, 783 (1997).
3. C. Kouveliotou et al., ApJ, 413, L101 (1993).
4. A.I. MacFadyen and S.E. Woosley, ApJ, 524, 262 (1999).
5. T. Piran, Phys. Rep., 314, 575 (1999).
6. L. Piro et al., ApJ, 514, L73 (1999).
7. L.A. Antonelli et al., ApJ, 545, L39 (2000).
8. L. Piro et al., Science, 290, 955 (2000).
9. L. Amati et al., Science, 290, 953 (2000).
10. J.N. Reeves et al., A&A, 403, 463 (2003).
11. N.R. Butler et al., ApJ, 597, 1010 (2003).
12. D. Watson et al., ApJ, 595, L29 (2003).
13. B.E. Schaefer et al., ApJ, 588, 387 (2003).
14. N. Mirabal et al., ApJ, 595, 935 (2003).
15. J. Heise et al., GCNC 1138 (2001).
16. J.S. Bloom, S.R. Kulkarni, S.G. Djorgovski, AJ, 123, 1111 (2002).
17. A.S. Fruchter et al., ApJ, 545, 664 (2000).
18. A.S. Fruchter et al., ApJ, 519, L13 (1999).
19. S.G. Djorgovski et al., ApJ, 562, 654 (2001).
20. J. Hjorth et al., ApJ, 576, 113 (2002).
21. S.G. Djorgovski, J.S. Bloom, S.R. Kulkarni, ApJ, 591, L13 (2003).
22. A.O. Jaunsen et al., A&A, 402, 125 (2003).
23. A.S. Fruchter et al., ApJ, 516, 683 (1999).
24. E. Le Floc'h et al., A&A, 400, 499 (2003).
25. J. Gorosabel et al., A&A, 400, 127 (2003).
26. J. Gorosabel et al., A&A, 409, 123 (2003).
27. L. Christensen et al., A&A, 413, 121 (2004).
28. S.R. Kulkarni et al., Nature, 393, 35 (1998).
29. J.S. Bloom et al., ApJ, 507, L25 (1998).
30. J. Hjorth et al., Nature, 423, 847 (2003).
31. J.P.U. Fynbo et al., A&A, 406, L63 (2003).
32. S.G. Djorgovski et al., in Gamma-Ray Bursts in the Afterglow Era, Proc. of the International Workshop held in Rome, Italy, 17–20 October 2000, Eds. E. Costa, F. Frontera, and J. Hjorth, p. 218 (astro-ph/0107535)
33. L. Christensen, J. Hjorth, J. Gorosabel, A&A, submitted (2004).
34. R. Chary, E.E. Becklin, L. Armus, ApJ, 566, 229 (2002).
35. D.A. Frail et al., ApJ, 565, 829 (2002).
36. E. Berger et al., ApJ, 588, 99 (2003).
37. D. Lazzati, S. Covino, G. Ghisellini, MNRAS, 330, 583 (2002).
38. M. De Pasquale et al., ApJ, 592, 1018 (2003).
39. S.A. Colgate, ApJ, 187, 333 (1974).
40. T.J. Galama et al., Nature, 395, 670 (1998).
41. S.R. Kulkarni et al., Nature, 395, 663 (1998).
42. S.E. Woosley et al., ApJ, 516, 788 (1999).
43. E. Pian et al., ApJ, 536, 778 (2000).
44. A.J. Castro-Tirado and J. Gorosabel, A&AS, 138, 449 (1999).
45. J.S. Bloom et al., Nature, 401, 453 (1999).
46. T.J. Galama et al., ApJ, 536, 185 (2000).
47. G. Björnsson et al., ApJ, 552, L121 (2001).
48. A.J. Castro-Tirado et al., A&A, 370, 398 (2001).
49. D. Lazzati et al., A&A, 378, 996 (2001).
50. J.S. Bloom et al., ApJ, 572, L45 (2002).
51. S. Dado, A. Dar, A. De Rujula, ApJ, 572, L143 (2002).
52. S. Dado, A. Dar, A. De Rujula, A&A, 393, L25 (2002).
53. P.M. Garnavich et al., ApJ, 582, 924 (2003).
54. P.A. Price et al., ApJ, 589, 838 (2003).
55. M. Della Valle et al., A&A, 406, L33 (2003).
56. J. Greiner et al., ApJ, 599, 1223 (2003).
57. N. Masetti et al., A&A, 404, 465 (2003).
58. S. Dado, A. Dar, A. De Rujula, ApJ, 593, 961 (2003).
59. S. Dado, A. Dar, A. De Rujula, ApJ, 594, L89 (2003).
60. P.A. Price and B.A. Peterson, GCNC 1987 (2003).
61. K. Torii et al., ApJ, 597, L101 (2003).
62. T. Matheson et al., ApJ, 599, 394 (2003).
63. K.Z. Stanek et al., ApJ, 591, L17 (2003).
64. K. Iwamoto et al., Nature, 395, 672 (1998).
65. P.A. Mazzali et al., ApJ, 599, L95 (2003).
66. S.E. Woosley and A. Heger, ApJ, submitted (astro-ph/0309165).
67. B. Paczyński, ApJ, 494, L45 (1998).
68. K. Iwamoto et al., ApJ, 534, 660 (2000).
69. P.A. Mazzali et al., ApJ, 545, 407 (2000).
70. P.A. Mazzali et al., ApJ, 572, L61 (2002).
71. W. Zhang et al., ApJ, 586, 356 (2003).
72. J.S. Bloom et al., ApJ, 599, 957 (2003).
73. A.M. Soderberg et al., ApJ, submitted (astro-ph/0311050).
74. J.P.U. Fynbo et al., in preparation (2004).
75. J. Granot et al., ApJ, 570, L61 (2002).
76. R. Sari and T. Piran, ApJ, 520, 641 (1999).